

In vivo characterization of myocardial infarction using fluorescence and diffuse reflectance spectroscopy

Yalin Ti*

Poching Chen

Wei-Chiang Lin[†]

Florida International University
Department of Biomedical Engineering
Miami, Florida 33199

Abstract. We explore the feasibility of using combined fluorescence and diffuse reflectance spectroscopy to characterize a myocardial infarct at different developing stages. An animal study is conducted using rats with surgically induced myocardial infarction (MI). *In vivo* fluorescence spectra at 337-nm excitation and diffuse reflectance between 400 and 900 nm are measured from the heart. Spectral acquisition is performed: 1. for normal heart tissue; 2. for the area immediately surrounding the infarct; and 3. for the infarcted tissue itself, one, two, three, and four weeks into MI development. Histological and statistical analyses are used to identify unique pathohistological features and spectral alterations associated with the investigated regions. The main alterations ($p < 0.05$) in diffuse reflectance spectra are identified primarily between 450 and 600 nm. The dominant fluorescence alterations are increases in peak fluorescence intensity at 400 and 460 nm. The extent of these spectral alterations is related to the duration of the infarction. The findings of this study support the concept that optical spectroscopy could be useful as a tool to noninvasively determine the *in vivo* pathophysiological features of a myocardial infarct and its surrounding tissue, thereby providing real-time feedback to surgeons during various surgical interventions for MI.
© 2010 Society of Photo-Optical Instrumentation Engineers. [DOI: 10.1117/1.3442505]

Keywords: myocardial infarction; diagnosis; diffuse reflectance spectroscopy; fluorescence spectroscopy.

Paper 09380R received Aug. 26, 2009; revised manuscript received Apr. 6, 2010; accepted for publication Apr. 7, 2010; published online Jun. 9, 2010.

1 Introduction

Myocardial infarction (MI) is the most severe type of ischemic myocardial injury. It is caused by the blockage of one or more than one coronary artery, and is the most prevalent form of coronary artery disease (CAD), with approximately 8 million Americans having experienced at least one MI.¹ Chronic MI can trigger a complicated tissue-remodeling process in the left ventricle, a process that often involves the progressive death of cardiomyocytes, tissue inflammation, the formation and remodeling of granulation tissue, and eventually, the maturation of scars within the zone of infarction.² The formation of an infarct also alters physiological conditions, such as blood flow pattern, and hence the functionality of the myocardium surrounding the infarct. This dysfunctional tissue is further classified clinically into stunned³⁻⁵ and hibernating^{6,7} myocardium, based on its pathophysiological features.

An accurate assessment of the degree of tissue damage induced by MI is critical for patient management; it aids clinicians to optimize treatment for each individual. Gaining such knowledge is equally important for researchers, because it facilitates the development of more effective MI treatments.^{8,9} While many hallmark pathological and physiological alterations appear in left ventricle myocardium post-MI, on-site real-time acquisition of such information remains unavailable in *in vivo* and intraoperative situations. Various clinical diagnostic technologies, such as contrast-enhanced magnetic resonance imaging (CMRI), positron emission tomography (PET), single photon emission computed tomography (SPECT), and NOGA[™] electromechanical mapping (Cordis Corporation, Bridgewater, New Jersey), have been used to assess myocardial tissue damage post infarction; the capabilities of these technologies in terms of detecting and grading infarcted myocardial tissue have been shown in various studies.¹⁰⁻¹⁹ However, the bulkiness and expensiveness of these imaging devices create sizable challenges with respect to incorporating them for intraoperative guidance during surgical interventions like angioplasty and stem cell implantation.

Optical spectroscopy offers the advantages of providing noninvasive, automated tissue characterization in real time, because it uses the interaction between light and tissue to

*Current affiliation: University of Pennsylvania, Departments of Physics and Astronomy, 3231 Walnut Street, Philadelphia, Pennsylvania, 19104, and University of Pennsylvania, School of Medicine, Department of Radiation Oncology, 3620 Hamilton Walk, Philadelphia, Pennsylvania, 19104; E-mail: yalinti@mail.med.upenn.edu

[†]Address all correspondence to: Wei-Chiang Lin, Department of Biomedical Engineering, Florida International University, 10555 W. Flagler Street EAS 2673, Miami, Florida 33199. Tel: 305-348-2112; Fax: 305-348-6954; E-mail: wclin@fiu.edu

detect alterations in tissue morphological and biochemical characteristics. The applicability of optical spectroscopy, fluorescence, and diffuse reflectance spectroscopy in particular in the detection of early-stage cancer has been demonstrated by several research groups.²⁰⁻²³ Reports on the use of optical spectroscopy to assess the hemodynamic and metabolic characteristics of *in vivo* tissue also can be found throughout the literature.^{21,22,24-28} The utility of optical spectroscopy in detecting tissue injuries and post-injury tissue remodeling has been explored in a limited fashion,²⁹⁻³² and this is especially true for MI.

In vivo applications of optical spectroscopy relevant to the heart are relatively few. Of those reported studies, many focus on using diffuse reflectance spectroscopy to gauge the hemodynamic characteristics of the heart.³³⁻³⁶ For example, Haggblad et al. estimate myocardial tissue oxygenation during a coronary artery bypass graft surgery using calibrated broadband diffuse reflectance spectroscopy in conjunction with a hand-held fiber optic probe.³⁴ Baykut et al. apply near-infrared spectroscopy to the determination of myocardial oxygenation status during myocardial ischemia induced by left anterior descending (LAD) ligation.³⁶ In addition, fluorescence spectroscopy is used to determine tissue viability and metabolic activities.³⁷⁻³⁹ While these studies demonstrate the potential intraoperative utilities of optical spectroscopy in determining certain short-term physiological alterations induced by ischemia, they do not address the possibility of using optical spectroscopy to evaluate the complex myocardial tissue remodeling processes induced by MI over a long period of time.

In this study, we explored the validity of using combined fluorescence and diffuse reflectance spectroscopy to characterize a myocardial infarct at different stages of its development. *In vivo* fluorescence and diffuse reflectance spectra were acquired from rat hearts post infarction using a fiber optic spectroscopic system. Spectral acquisition was performed on the infarct as well as on its surrounding area. Acquired spectra were analyzed using statistical tools to exploit the unique spectral features associated with the pathophysiological characteristics of infarcted myocardial tissue determined using the histological method.

2 Methods

2.1 Animal Preparation

The study protocol reported next was reviewed and approved by the Institutional Animal Care and Use Committee at Florida International University, Miami. The animal model utilized in this study was the Sprague-Dawley rat model of MI, and these rats were purchased from Charles River Laboratories (Wilmington, Massachusetts). The mechanism of MI induction used by Charles River Laboratories was ligation of the left anterior descending (LAD) coronary artery by means of a cranial-caudal incision. Initially, purchased rats generally weighed approximately 200 g. On arrival, the rats were housed within a local animal care facility for one, two, three, or four weeks, depending on the intended infarct development duration, during which they were provided with normal food and water.

Prior to the optical characterization study, the rats were prepared in accordance with the following procedures. Each

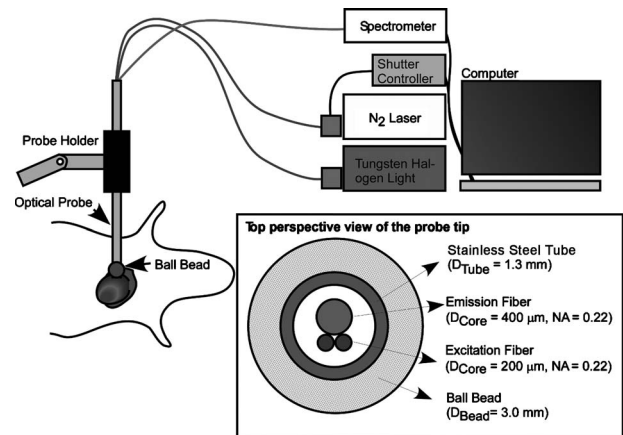


Fig. 1 Schematic of the spectroscopic system and the experiment setup.

rat initially was sedated using isoflurane vapor, followed by a sodium pentobarbital (50 mg/kg) injection. The anesthetized rat was transported to an operating table and connected to a nosecone, through which a 2.5% isoflurane-oxygen mixture was administered. The chest of the rat was shaved and disinfected using povidone iodine. A tracheotomy then was performed with a 14-gauge IV catheter inserted into the trachea, so that a respirator could be connected to regulate the rat's breathing rate (50 breaths/min) and volume (1 L/min). Thereafter, a 1.5% isoflurane-oxygen mixture was administered to maintain a constant level of anesthesia for the duration of the experiment. To avoid any over- or underdosing of isoflurane, the rat's heart rate was monitored constantly. The anesthetized rat was placed in the supine position and its heart exposed by means of a median sternotomy. Then the heart, especially the left ventricle, was photographed to document its gross appearance.

2.2 Instrumentation

A fiber optic fluorescence and diffuse reflectance spectroscopic system was used to perform *in vivo* optical characterization (Fig. 1). The system utilized a 337 nm nitrogen-dye laser (VLS-337, Spectra-Physics, Mountain View, California) for fluorescence spectroscopy, and a tungsten-halogen white light source (LS-1, OceanOptics, Dunedin, Florida) for diffuse reflectance spectroscopy. The energy level of the laser light delivered to the targeted tissue was $\sim 0.02 \mu\text{J}/\text{pulse}$, and the power level of the white light $\sim 0.025 \text{ mW}$. These light energy and power levels were much lower than the safety level established by the American National Standards Institute (ANSI) and should not cause any photothermal damage to the targeted tissue. Spectral detection was achieved using a miniature fiber optic spectrometer (USB 2000, OceanOptics, Dunedin, Florida) with a $100 \mu\text{m}$ entrance slit. The spectrometer has a detection range of 250 to 932 nm and a spectral resolution of 5 nm. Excitation light delivery and emission light detection were carried out using a fiber optic probe. The fiber optic probe was developed and built in-house, and it consisted of three fibers placed in a microstainless steel tube with an outer diameter of 1.3 mm. Two fibers with a $200 \mu\text{m}$ core diameter were used for laser light and

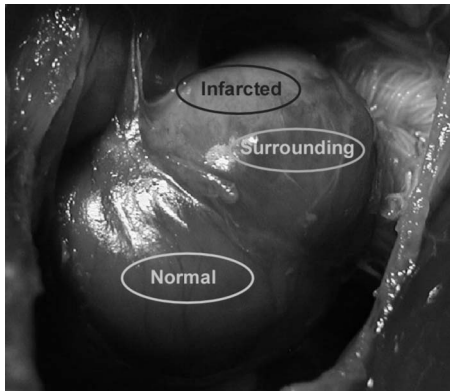


Fig. 2 Representative tissue regions for optical measurement.

white light conduction; one fiber with a 400 μm core diameter was used for detection of both fluorescence light and diffuse reflectance light. To avoid any tissue damage induced by the sharp edge of the stainless steel tube, a 3 mm diameter black spherical bead was placed at the tip of the probe. This approach also increased the contact area of the probe, which reduced the risk of spectral artifacts induced by excessive probe contact pressure.⁴⁰ Note that the probe was inserted through the center hole of the bead, so the bead did not introduce any unwanted spectral alterations. The fiber optic probe was held in position by a mechanical arm, which limited probe mobility to its axial direction. During each spectral acquisition procedure, the optical probe was placed perpendicular to the tissue surface. Because of gravity, the tip of the probe would remain in constant contact with the tissue site being investigated.

2.3 Data Collection

Fluorescence and diffuse reflectance spectra were acquired from the normal myocardium (normal control), as well as from the infarct and its surrounding tissue. Measurements were categorized by region, subdivided into 1. normal region, 2. infarcted region, and 3. surrounding region (i.e., tissue surrounding the infarct) (Fig. 2), based on the visual observations of the operators. Since the development of infarction was individually different, the extensively whitened area, a result of low blood flow and/or collagen formation, was first identified and denoted as the infarcted region. The surrounding region was defined as the tissue area within 5 mm of the boundary of the infarcted region. Consequently, given that we already had demonstrated that *in vivo* fluorescence and diffuse reflectance spectra from the right and left ventricle are similar in an earlier separate study, normal control measurements were performed on the right ventricle. From a single investigated site, more than four sets of optical spectra were acquired for the purpose of demonstrating the reproducibility of measurements. The integration time used in a single spectral acquisition was maintained at one second. The probe tip was rinsed and the investigated sites cleaned and irrigated using a saline solution between measurements. A total of eight or more investigated sites were selected from each studied rat. At the end of the optical characterization study, the rat was euthanized by injecting saturated potassium chloride directly into its right ventricle. The investigated sites were registered using

a digital camera and 38 gauge acupuncture needles post euthanization. The small needle size minimized the physical damage introduced during the site registration procedure. The heart was removed from the dead rat and fixed in 4% formalin for histological examination.

2.4 Data Analysis

All acquired spectra were processed using a Savitzky-Golay filter to eliminate any high frequency noise originating from the spectrometer itself. The filtered spectra $I_{\text{raw}}(\lambda)$ were processed to remove those spectral alterations induced by ambient light $B(\lambda)$ and intrinsic instrumentation characteristics $C(\lambda)$. That is,

$$I(\lambda) = [I_{\text{raw}}(\lambda) - B(\lambda)] \times C(\lambda), \quad (1)$$

where $I(\lambda)$ represents a calibrated spectrum. The derivation of $C(\lambda)$, also known as the *calibration factor*, can be found in a previous publication.⁴¹ The spectral ranges of the calibrated spectra were limited to 380 to 750 nm and 400 to 900 nm for fluorescence spectra and diffuse reflectance spectra, respectively. To facilitate data processing and analysis, the spectra were resampled at 5 nm intervals.

Spectral analysis was performed with the calibrated spectra to identify and quantify those spectral alterations induced by MI. The mean fluorescence and diffuse reflectance spectra of a single investigated site were calculated from the repeated measurements and used as representatives. The average of the maximum intensities were calculated using the mean spectra from the normal region within a single rat study; they were then used as the bases to which the spectra from the surrounding and infarcted regions were normalized. This data normalization procedure minimized the effects of biological variations in the absolute quantity of spectral alterations among all rat studies. The normalized spectra from the entire study were divided into three subgroups based on measurement region (i.e., normal, infarcted, and surrounding regions). Within each group, the spectra were further subdivided relative to the duration of the MI development (i.e., one, two, three, or four weeks).

Two spectral analysis procedures were deployed to evaluate alterations in both the normalized spectral profile and intensity induced by the infarct development. In addition, the two parameters—investigated location and infarct development duration—were analyzed, both separately and together, in terms of their effects on spectral alterations. Initial analyses were conducted using empirical methods, with spectral alterations between different spectral groups identified by an experienced observer. Furthermore, statistical tools were used to determine the significance of these spectral alterations. Statistic analysis of the data was tailored based on the distribution and variance characteristics of the data. The normality of the data was determined by Lilliefors test initially. Parametric statistical analysis [i.e., one way analysis of variance (ANOVA)] was used for datasets with large sample size and normal distribution characteristics; nonparametric statistical analysis (i.e., Kruskal-Wallis analysis of ranks) was used for datasets with small sample size and/or non-normal distribution characteristics. Following the initial statistical comparisons among all groups, Tukey's least significant difference procedure was

Table 1 Summary of the number and distribution of the investigated sites.

	Week 1	Week 2	Week 3	Week 4
Number of rats	5	5	5	5
Number of investigated sites				
Normal region	16	18	14	16
Surrounding region	11	13	14	16
Infarcted region	11	16	13	17

used to identify the differences within any two groups. All data processing and analysis codes were developed using MATLAB 7.5.

2.5 Histopathological Examination

For each investigated site, a tissue specimen of about 1 mm diameter and 3 to 5 mm thickness was obtained and stored in formalin. The preserved tissue specimens were embedded in paraffin blocks. From each block, four consecutive four-micron sections were cut and then stained using hematoxylin and eosin. The prepared tissue slides were evaluated by a histologist who was blinded to all spectroscopic study results. In addition to identifying the histological features associated with MI, the histologist also reported on the extent of the features.

3 Results

Optical investigations were conducted using five rats for each duration of the MI development (i.e., one, two, three, and four weeks), with multiple measurements performed at investigated sites randomly selected from the normal, surrounding, and infarcted regions. Summary data on the number and distribution of the investigated sites are provided in Table 1.

3.1 Histological Examination

Histological examination results for the tissue specimens from the normal, surrounding, and infarcted regions are listed in Table 2. The number of tissue samples was less than the number of investigated sites, because only one tissue specimen was collected when two investigated sites were immediately adjacent. The primary histopathological features observed in the specimens from surrounding and infarcted tissue included vascular/epicardial inflammation, myocardial inflammation, and myocardial fibrosis (Fig. 3), with their extents varying from focal, to multifocal, to confluent and diffuse. Histological analysis revealed that the normal samples primarily were composed of healthy myocardium, with some displaying mild histological features of inflammation, such as vascular/epicardial and myocardial inflammation. Specimens collected from the surrounding region exhibited a more significant inflammatory response and a minimal to mild degree of myofibrosis. Specimens from the infarcted region displayed severe inflammation and confluent myofibrosis. Although not preva-

Table 2 Summary of histological examination results.

Feature	Location		
	Normal (n=43)	Surrounding (n=40)	Infarcted (n=38)
Normal conditions	24	8	3
Vascular inflammation	12	19	21
Myocardial inflammation	11	19	26
Myofibrosis	Minimal	2	4
	Mild	1	5
	Severe	0	5

lent, various levels of myocardial degeneration/loss and hemorrhage were found in some tissue specimens from the surrounding and infarcted regions.

3.2 Spectral Analysis

Since all spectra were normalized to their corresponding normal references, the spectral variations among all normal references (i.e., original calibrated spectra from the normal region) were compared. The results of comparisons show that no significant differences in either intensity or profile existed in either fluorescence or diffuse reflectance spectra from the normal regions of the hearts at weeks 1, 2, 3, or 4 (data not shown). This indicates that the normal references used in this study were not affected by the infarct development duration. Several spectral alterations, however, were observed in the fluorescence and diffuse reflectance spectra acquired from the surrounding and infarcted regions, in comparison with their corresponding normal references for the same week. It was apparent that the alterations in fluorescence and diffuse reflec-

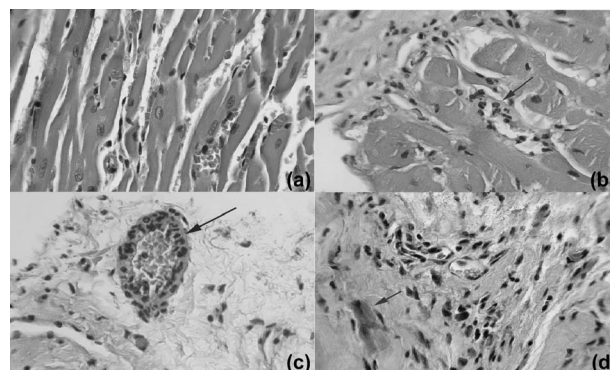


Fig. 3 The primary histopathological features observed in the myocardial specimens from the surrounding and infarcted regions: (a) normal appearing myocardium; (b) minimal neutrophilic myocardial inflammation and early myofiber degeneration (arrow); (c) typical vascular inflammation (epicardial and myocardial) with neutrophils (arrow) and minimal loss of vascular integrity; and (d) severe myocardial inflammation and fibrosis with mononuclear inflammatory cells and myofiber fragment (arrow).

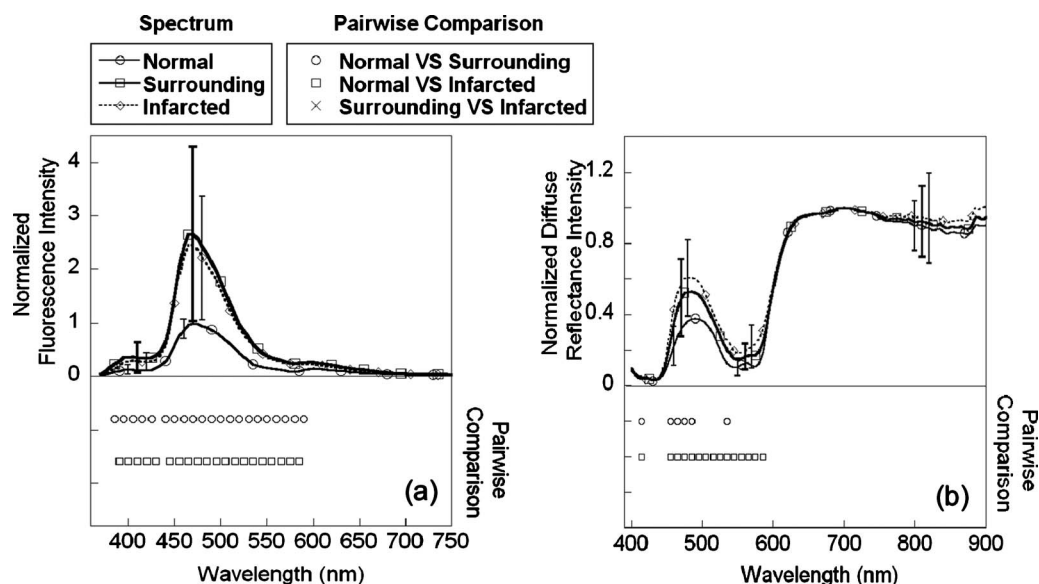


Fig. 4 Region-specific comparison of *in vivo* (a) fluorescence and (b) diffuse reflectance spectra from the rat hearts one week after the MI induction surgery. The symbols below the spectral plots show the outcomes of the pair-wise comparison between any two groups at each wavelength. The statistical significance level was set at 0.05 in this study.

tance spectra were modulated by both the development durations of an infarct and the investigated location.

3.2.1 Week 1 comparisons

The fluorescence spectra acquired from normal myocardium exhibited one dominant peak at ~ 470 nm emission and two secondary peaks at 400 and 600 nm [Fig. 4(a)]. These features were consistent across all MI development durations. For the fluorescence spectra obtained from the surrounding and infarcted regions, the most noticeable change was an increase in intensity at ~ 470 nm ($p < 0.05$), which averaged about 150% above that obtained from normal tissue. No appreciable difference in terms of the magnitude was found between the spectra from the surrounding region and those from the infarcted region at week 1. Moreover, the fluorescence profile characteristics for all three tissue regions were similar.

The diffuse reflectance spectra from the normal region exhibited trademark oxyhemoglobin and oxymyoglobin absorption in the visible wavelength region (i.e., a double valley between 500 and 600 nm), and a monotonic decreasing trend beyond 650 nm [Fig. 4(b)]. Diffuse reflectance spectra from the surrounding and infarcted regions revealed mild elevation in intensity between 450 and 600 nm ($p < 0.05$), where the most prominent increase was found at 480 nm. Moreover, diffuse reflectance spectra from the infarcted region showed hallmark absorption characteristics of deoxyhemoglobin and deoxymyoglobin: a single valley between 500 and 600 nm. Comparisons of diffuse reflectance spectra from the infarcted and surrounding regions yielded no statistically significant differences within this data subset.

3.2.2 Week 2 comparisons

The comparisons performed on week-2 fluorescence spectra yielded conclusions similar to those drawn from week-1 data. Two additional features were identified in the fluorescence spectra from infarcted region [Fig. 5(a)]. First, fluorescence

emission at ~ 390 nm became prominent. Second, the primary emission peak shifted toward a shorter wavelength (470 to 460 nm, a blue-shift). A significant increase in diffuse reflectance intensity between 400 and 800 nm was detected in both the infarcted and surrounding regions, with the greatest increase found in the infarcted region [Fig. 5(b)]. The single valley profile between 500 and 600 nm, as mentioned before, only appeared in the diffuse reflectance spectra obtained from surrounding tissue. In addition, the decreasing trend in the diffuse reflectance spectra from the infarcted tissue between 700 and 900 nm was more pronounced than that observed for either the normal or surrounding regions.

3.2.3 Week 3 comparisons

Comparisons of the week-3 fluorescence spectra led to the same observations derived from the week-2 comparisons, with one exception: the blue-shift in the fluorescence peak from infarcted tissue was no longer noticeable [Fig. 6(a)]. In terms of diffuse reflectance spectra, a statistically significant elevation between 400 and 600 nm only was detectable in infarcted tissue [Fig. 6(b)]. The average diffuse reflectance spectra from the three regions did not possess the single valley characteristic between 500 and 600 nm observed in weeks 1 and 2.

3.2.4 Week 4 comparisons

The fluorescence spectra observed in infarcted tissue again were significantly different than those from normal or surrounding tissue [Fig. 7(a)]. The average fluorescence intensity at ~ 470 nm was approximately 1.5 times greater in infarcted tissue versus normal tissue. The peak at 400 nm was as prominent as that at 470 nm in the fluorescence spectra from infarcted tissue. While the average fluorescence emission from surrounding tissue was greater than from normal, this difference was not statistically significant across the majority of the wavelength region. In the diffuse reflectance spectra, a

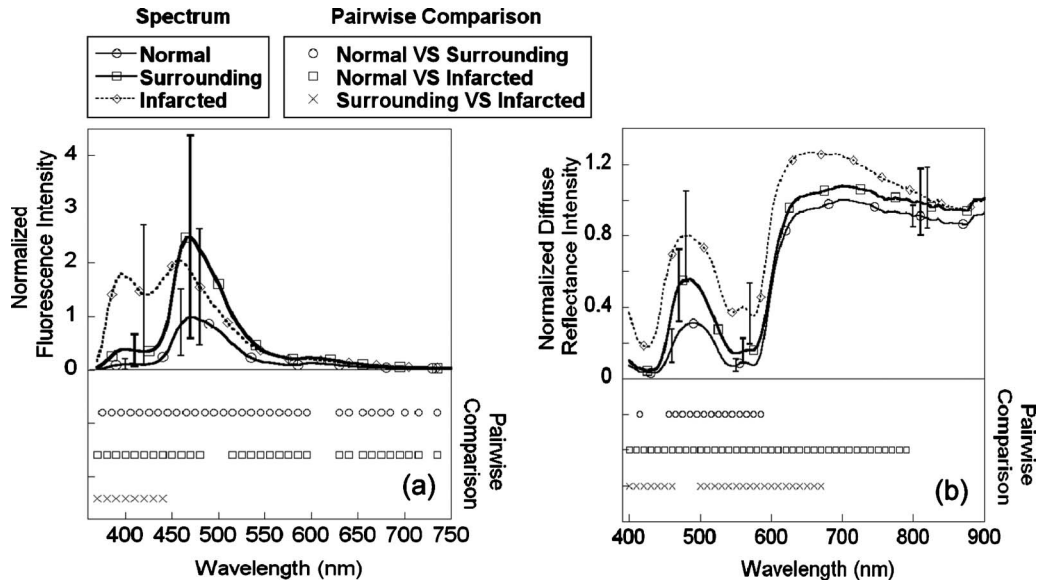


Fig. 5 Region-specific comparison of *in vivo* (a) fluorescence and (b) diffuse reflectance spectra from the rat hearts two weeks after the MI induction surgery. The symbols below the spectral plots show the outcomes of the pair-wise comparison between any two groups at each wavelength. The statistical significance level was set at 0.05 in this study.

significant elevation in diffuse reflectance intensity between 400 to 600 nm remained in the infarcted region [Fig. 7(b)]. The average diffuse reflectance spectra from normal and surrounding regions were almost identical.

4 Discussion

Using histological methods, we are able to gain insights into the remodeling process of myocardial tissue post infarction. The primary microscopic features that we detected are associated with 1. inflammation, specifically vascular and myocardial inflammation, and 2. wound healing in the form of myo-

fibrosis. Vascular and myocardial inflammation are observed frequently in the area surrounding an infarct, while myofibrosis is located within the infarcted tissue itself. Meanwhile and predictably, normal tissue samples mainly exhibit healthy myocardium, though some display of mild vascular/epicardial inflammation and myocardial inflammation is evident. This may indicate the occurrence of bacterial or viral infection in the entire heart after an infarction.

Spectral analysis revealed significant differences in the fluorescence and diffuse reflectance spectra across the three different tissue regions we evaluated (normal tissue, infarcted

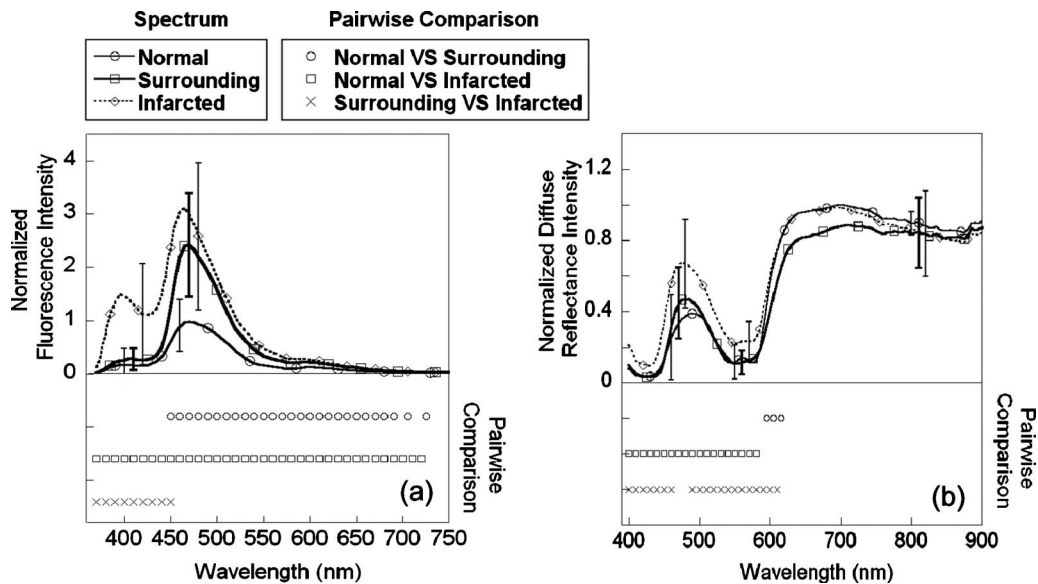


Fig. 6 Region-specific comparison of *in vivo* (a) fluorescence and (b) diffuse reflectance spectra from the rat hearts three weeks after the MI induction surgery. The symbols below the spectral plots show the outcomes of the pair-wise comparison between any two groups at each wavelength. The statistical significance level was set at 0.05 in this study.

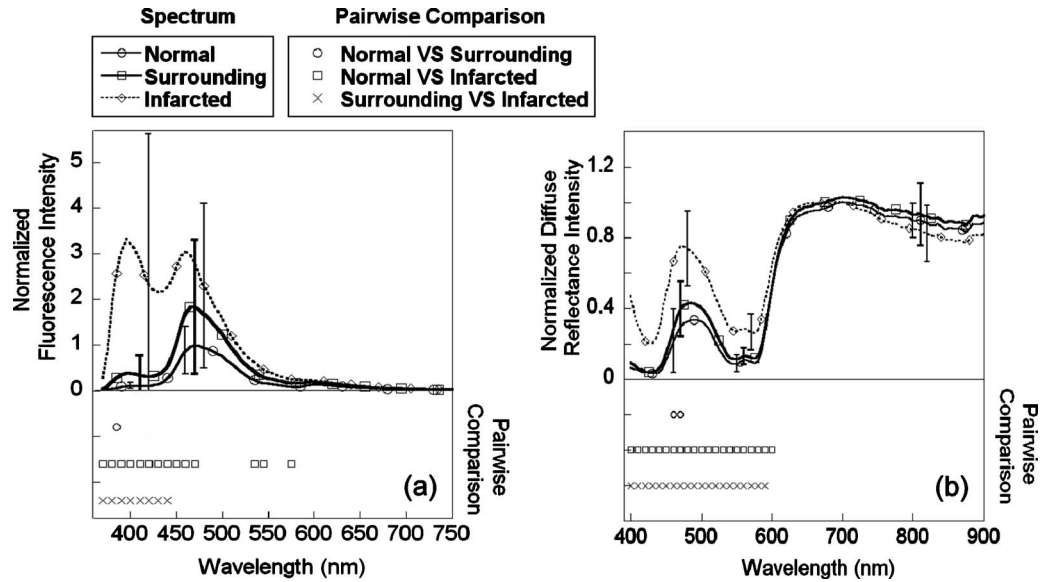


Fig. 7 Region-specific comparison of *in vivo* (a) fluorescence and (b) diffuse reflectance spectra from the rat hearts four weeks after the MI induction surgery. The symbols below the spectral plots show the outcomes of the pair-wise comparison between any two groups at each wavelength. The statistical significance level was set at 0.05 in this study.

tissue, and the tissue immediately surrounding an infarct). Moreover, the presence and magnitude of these spectral alterations appear to be sensitive to the length of time post infarction.

The statistically significant alterations ($p < 0.05$) in diffuse reflectance spectra are found primarily between 450 and 600 nm, with spectral profile alterations between 500 and 600 nm and an intensity alteration at ~480 nm especially prominent. Since diffuse reflectance signals within this spectral band are heavily influenced by two key chromophores in myocardium, namely hemoglobin and myoglobin, the spectral alterations reported may be attributed primarily to alterations in local hemodynamics, including reductions in the oxygenation of hemoglobin/myoglobin and local blood volume, which occur during an MI. The double valley characteristic identified in the diffuse reflectance spectra between 500 and 600 nm in normal myocardium is caused by the twin absorption peaks of oxyhemoglobin and oxymyoglobin across the same spectral region. These absorption peaks stem from the oxy- α and oxy- β bindings of hemoglobin and myoglobin.⁴²⁻⁴⁴ Deoxyhemoglobin and deoxymyoglobin, on the other hand, possess only a single absorption peak at 570 nm, due to the conformational changes led by the cooperative ligand binding.⁴⁵ Therefore, a significant decrease in the oxygenation of myocardial tissue would be expected to lead to a unique spectral profile alteration in diffuse reflectance spectra: the double valley feature between 500 and 600 nm is replaced by a single valley one (Fig. 8). This alteration is most prominent among the diffuse reflectance spectra collected from infarcted tissue and its surroundings one-week post infarction. The deoxygenation in the infarcted region at week 1 is the direct result of the reduction of regional blood flow post. Although neovascularization recovers the basal coronary flow within one week post infarction, the maximal coronary flow was not normalized until 35 days later. Only 25% of the maximal left ventricular flow is received at the center of the infarcted

area.⁴⁶ The deoxygenation in the surrounding region one week after inducing myocardial infarction may be due to the reduced blood flow in this area, in which the hibernating myocardium with contractile dysfunction is usually found (perfusion-contraction matching).⁴⁷⁻⁵⁰ However, there is still debate regarding whether the chronically reduced blood flow is a cause or consequence of chronic myocardial hibernation.⁵¹ According to the results of this study, this double valley reappears in diffuse reflectance spectra from both the infarcted and surrounding regions two weeks post infarction, suggesting some recovery of tissue oxygenation. However, the distortion of the observed double valley profile indicates a tissue oxygenation level that is not fully restored within the infarcted and surrounding regions.

Diffuse reflectance intensities at isosbestic points, like 550 and 570 nm, can be used to monitor blood volume in the tissue because, at these wavelengths, the absorption properties

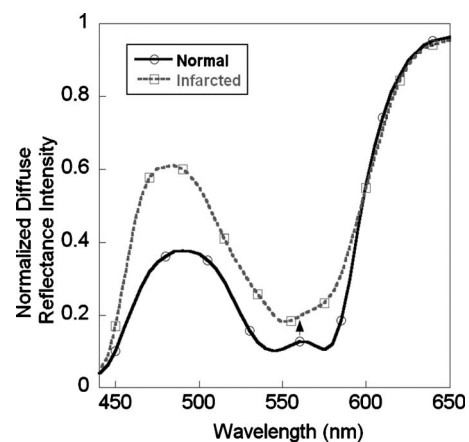


Fig. 8 The corresponding spectral profile alteration in diffuse reflectance spectra related to the change in hemo/myoglobin oxygenation.

of the two major moieties of hemoglobin are uninfluenced by their oxidation state. In this study, we notice that diffuse reflectance intensities at 480, 550, and 570 nm in both infarcted tissue and the tissue immediately surrounding it often are higher than in normal myocardium. This phenomenon indicates that the infarct and its surrounding area have reduced blood volume, which also means reduced hemoglobin and myoglobin content. The reduced blood volume that is characteristic of infarcted tissue persists for at least the first four weeks after an infarction.

Diffuse reflectance spectra from all three tissue regions exhibit a descending trend between 600 and 900 nm. In this spectral region, the predominant contributor to the diffuse reflectance signals of biological tissue is its scattering properties. Consequently, this trend toward decline might be explained by the wavelength dependence of elastic scattering using Mie's theory,^{22,52} where the scattering property decreases as the wavelength increases. We note that diffuse reflectance from the infarcted region has a distinctive increase in this spectral region two weeks post infarction, which is not observed in the other regions. While not yet elucidated, we believe that one potential explanation for this phenomenon is the formation of granulation tissue, a process that generally takes place two to three weeks after infarction. The 2- to 3-week-old granulation tissue is rich in cross-linked interstitial collagens, myofibroblasts, macrophages, and small blood vessels; all of these features could contribute to an increase in the concentration of tissue scatterers, and hence, elevation of the diffuse reflectance signals. However, this granulation only transpires for a short period of time, as the total cell number in granulation tissue decreases during scar maturation.²

One dominant fluorescence alteration observed in this study is the increase in fluorescence intensity around 460 nm. This feature often coexists with the presence of deoxyhemoglobin and deoxymyoglobin characteristics in diffuse reflectance spectra. In accordance with the fluorescence characteristics of biological fluorophores, it is believed that the main source of fluorescence emission at 460 nm from biological tissue is NAD(P)H. The shortage in oxygen supply in the area of infarction leads to a reduction in the metabolic rate, and hence, the accumulation of NAD(P)H. This, in turn, leads to a significant increase in tissue fluorescence at 337 nm excitation. This phenomenon is seen commonly in fluorescence spectroscopy for *in vivo* tissue diagnosis, which is why fluorescence spectroscopy is used frequently as a nondestructive tool for monitoring tissue metabolic activity. The fluorescence increase phenomenon may also be attributed to the change in the absorption properties of the tissue. Infarction often reduces the fractional blood volume and oxygenation of the myocardial tissue, which leads directly to a decrease in the absorption properties of the tissue between 450 and 500 nm. Such an event would impact the observed fluorescence in two ways: it will increase the local fluence rate of the excitation light and reduce the attenuation of the photons associated with the fluorescence. In combination, these effects enhance the fluorescence from the investigated tissue. The phenomenon of increased peak fluorescence intensity observed in the tissue surrounding the infarct fades away as the infarct develops, as detected in the fluorescence spectra during weeks 3 and 4 post

infarction. This trend could be explained by the recovery of hemodynamics in the surrounding region. This interpretation matches the pathological alterations that have been described for hibernating myocardium.^{6,7,53}

Another fluorescence spectral feature that was observed in this study is an emission peak at 400 nm. While its magnitude varies, this feature is identified commonly in both infarcted and surrounding tissue one week post infarction. The presence of this fluorescence emission peak may be attributed to two biofluorophores found in the extracellular matrix of cardiac myocytes, fibrin, and collagen; both fluorophores produce strong 400 nm emission when excited by 340 nm light.⁵⁴ In the infarcted tissue, this emission peak becomes so dominant that it alters the fluorescence spectral profile into a single peak at ~400 nm. This phenomenon is the result of collagen cross-link proliferation, leading to scar formation.²

One key challenge faced when using the previously mentioned optical spectroscopy system to characterize a myocardial infarct *in vivo* is movement of the heart. In particular, beating of the heart can alter the contact point of the fiber optic probe, thereby changing the location of the investigation during a single spectral acquisition procedure. This problem is exacerbated by the fact that the normal heart rate of a rat is about 300 beats per minute. Therefore, large discrepancies frequently were observed between repeat spectra acquired from a single investigated site, especially within the tissue region surrounding an infarct. This also implies that more representative spectral features associated with infarction-induced myocardial tissue remodeling might be observed if the motion artifact could be removed from the spectral acquisition procedure. Furthermore, movement of the heart also modulates probe contact pressure, potentially inducing local tissue ischemia, and hence, alterations in the acquired spectra. On the other hand, during a previous study,⁴⁰ we found that the contact pressure induced by the fiber optic probe in this study was not sufficiently heavy to induce local ischemia in heart tissue. Consequently, we believe that the deoxyhemoglobin and deoxymyoglobin features we observed in this study represent intrinsic tissue characteristics.

Although optical spectroscopy has been used to diagnose the tissue conditions of various organs, there is no particular information available, to date, on its capacity to discriminate between the different tissue conditions of myocardium across various stages of MI. Being able to differentiate affected but still viable myocardium (i.e., stunned and hibernating myocardium) from both normal and infarcted myocardium is of great clinical importance. This rat study has provided meaningful information on tissue differentiation after MI induction. It is our intention to now extend the current study protocol to a rabbit model, which is more morphologically and pathologically similar to the human heart,⁵⁵ and hence may serve as a key stepping stone toward future human clinical trials.

Acknowledgments

Financial support from the American Heart Association (0655392B) and the Ware Foundation Research Endowment is gratefully acknowledged. We are indebted to Rafael O. Vidaud and Robert E. Schmidt for their assistance on animal surgical procedures and histological examination.

References

- W. Rosamond, K. Flegal, G. Friday, K. Furie, A. Go, K. Greenlund, N. Haase, M. Ho, V. Howard, B. Kissela, S. Kittner, D. Lloyd-Jones, M. McDermott, J. Meigs, C. Moy, G. Nichol, C. J. O'Donnell, V. Roger, J. Rumsfeld, P. Sorlie, J. Steinberger, T. Thom, S. Wasserthiel-Smoller, and Y. Hong, "Heart disease and stroke statistics—2007 update: a report from the American Heart Association Statistics Committee and Stroke Statistics Subcommittee," *Circulation* **115**(5), e69–171 (2007).
- W. M. Blankesteyn, E. Creemers, E. Lutgens, J. P. Cleutjens, M. J. Daemen, and J. F. Smits, "Dynamics of cardiac wound healing following myocardial infarction: observations in genetically altered mice," *Acta Physiol. Scand.* **173**(1), 75–82 (2001).
- R. Bolli, "Basic and clinical aspects of myocardial stunning," *Prog. Cardiovasc. Dis.* **40**(6), 477–516 (1998).
- E. Braunwald and R. A. Kloner, "The stunned myocardium: prolonged, postischemic ventricular dysfunction," *Circulation* **66**(6), 1146–1149 (1982).
- J. D. Schipke, B. Korbmayer, A. Dorszewski, G. Selcan, U. Sunderdiek, and G. Arnold, "Haemodynamic and energetic properties of stunned myocardium in rabbit hearts," *Heart* **75**(1), 55–61 (1996).
- S. H. Rahimtoola, G. La Canna, and R. Ferrari, "Hibernating myocardium: another piece of the puzzle falls into place," *J. Am. Coll. Cardiol.* **47**(5), 978–980 (2006).
- R. Schulz and G. Heusch, "Hibernating myocardium," *Heart* **84**(6), 587–594 (2000).
- P. Menasche, "Myoblast transplantation: feasibility, safety and efficacy," *Ann. Med.* **34**(5), 314–315 (2002).
- D. A. Taylor, "Cell-based myocardial repair: how should we proceed?" *Int. J. Cardiol.* **95**(Suppl 1), S8–12 (2004).
- A. Wagner, H. Mahrholdt, T. A. Holly, M. D. Elliott, M. Regenfus, M. Parker, F. J. Klocke, R. O. Bonow, R. J. Kim, and R. M. Judd, "Contrast-enhanced MRI and routine single photon emission computed tomography (SPECT) perfusion imaging for detection of subendocardial myocardial infarcts: an imaging study," *Lancet* **361**(9355), 374–379 (2003).
- D. R. Tomlinson, H. Becher, and J. B. Selvanayagam, "Assessment of myocardial viability: comparison of echocardiography versus cardiac magnetic resonance imaging in the current era," *Heart, Lung Circ.* **17**(3), 173–185 (2008).
- B. Ozben, A. A. Cincin, and B. Mutlu, "Assessment of myocardial viability with cardiac magnetic resonance imaging," *Anadolu. Kardiyol. Derg.* **8**(Suppl 2), 71–76 (2008).
- R. Ouwkerk, P. A. Bottomley, M. Solaiyappan, A. E. Spooner, G. F. Tomaselli, K. C. Wu, and R. G. Weiss, "Tissue sodium concentration in myocardial infarction in humans: a quantitative ^{23}Na MR imaging study," *Radiology* **248**(1), 88–96 (2008).
- E. Nagel, C. Klein, I. Paetsch, S. Hettwer, B. Schnackenburg, K. Wegscheider, and E. Fleck, "Magnetic resonance perfusion measurements for the noninvasive detection of coronary artery disease," *Circulation* **108**(4), 432–437 (2003).
- G. Korosoglou, A. Hansen, J. Hoffend, G. Gavriloic, D. Wolf, J. Zehelein, U. Haberkorn, and H. Kuecherer, "Comparison of real-time myocardial contrast echocardiography for the assessment of myocardial viability with fluorodeoxyglucose-18 positron emission tomography and dobutamine stress echocardiography," *Am. J. Cardiol.* **94**(5), 570–576 (2004).
- R. J. Kim, R. M. Judd, E. L. Chen, D. S. Fieno, T. B. Parrish, and J. A. Lima, "Relationship of elevated ^{23}Na magnetic resonance image intensity to infarct size after acute reperfused myocardial infarction," *Circulation* **100**(2), 185–192 (1999).
- R. Hoffmann, H. Lethen, T. Marwick, M. Arnese, P. Fioretti, A. Pingitore, E. Picano, T. Buck, R. Erbel, F. A. Flachskampf, and P. Hanrath, "Analysis of interinstitutional observer agreement in interpretation of dobutamine stress echocardiograms," *J. Am. Coll. Cardiol.* **27**(2), 330–336 (1996).
- M. Carlsson, H. Arheden, C. B. Higgins, and M. Saeed, "Magnetic resonance imaging as a potential gold standard for infarct quantification," *J. Electrocardiol.* **41**(6), 614–620 (2008).
- J. J. Bax, D. Poldermans, A. Elhendy, E. Boersma, and S. H. Rahimtoola, "Sensitivity, specificity, and predictive accuracies of various noninvasive techniques for detecting hibernating myocardium," *Curr. Probl Cardiol.* **26**(2), 147–186 (2001).
- I. J. Bigio and S. G. Bown, "Spectroscopic sensing of cancer and cancer therapy: current status of translational research," *Cancer Biol. Ther.* **3**(3), 259–267 (2004).
- N. Ramanujam, "Fluorescence spectroscopy of neoplastic and non-neoplastic tissues," *Neoplasia* **2**(1–2), 89–117 (2000).
- R. Richards-Kortum and E. Sevick-Muraca, "Quantitative optical spectroscopy for tissue diagnosis," *Annu. Rev. Phys. Chem.* **47**, 555–606 (1996).
- K. Sokolov, M. Follen, and R. Richards-Kortum, "Optical spectroscopy for detection of neoplasia," *Curr. Opin. Chem. Biol.* **6**(5), 651–658 (2002).
- A. Mayevsky and G. G. Rogatsky, "Mitochondrial function *in vivo* evaluated by NADH fluorescence: from animal models to human studies," *Am. J. Physiol.: Cell Physiol.* **292**(2), C615–640 (2007).
- A. A. Stratonnikov and V. B. Loschenov, "Evaluation of blood oxygen saturation *in vivo* from diffuse reflectance spectra," *J. Biomed. Opt.* **6**(4), 457–467 (2001).
- J. Q. Brown, L. G. Wilke, J. Geradts, S. A. Kennedy, G. M. Palmer, and N. Ramanujam, "Quantitative optical spectroscopy: a robust tool for direct measurement of breast cancer vascular oxygenation and total hemoglobin content *in vivo*," *Cancer Res.* **69**(7), 2919–2926 (2009).
- B. Chance, Z. Zhuang, C. UnAh, C. Alter, and L. Lipton, "Cognition-activated low-frequency modulation of light absorption in human brain," *Proc. Natl. Acad. Sci. U.S.A.* **90**(8), 3770–3774 (1993).
- H. Mitsuta, H. Ohdan, Y. Fudaba, T. Irei, H. Tashiro, T. Itamoto, and T. Asahara, "Near-infrared spectroscopic analysis of hemodynamics and mitochondrial redox in right lobe grafts in living-donor liver transplantation," *Am. J. Transplant* **6**(4), 797–805 (2006).
- K. A. Horvath, K. T. Schomacker, C. C. Lee, and L. H. Cohn, "Intraoperative myocardial ischemia detection with laser-induced fluorescence," *J. Thorac. Cardiovasc. Surg.* **107**(1), 220–225 (1994).
- W. C. Lin, A. Mahadevan-Jansen, M. D. Johnson, R. J. Weil, and S. A. Toms, "In vivo optical spectroscopy detects radiation damage in brain tissue," *Neurosurgery* **57**(3), 518–525 (2005).
- C. R. Buttemere, R. S. Chari, C. D. Anderson, M. K. Washington, A. Mahadevan-Jansen, and W. C. Lin, "In vivo assessment of thermal damage in the liver using optical spectroscopy," *J. Biomed. Opt.* **9**(5), 1018–1027 (2004).
- D. C. Morgan, J. E. Wilson, C. E. MacAulay, N. B. MacKinnon, J. A. Kenyon, P. S. Gerla, C. Dong, H. Zeng, P. D. Whitehead, C. R. Thompson, and B. M. McManus, "New method for detection of heart allograft rejection: validation of sensitivity and reliability in a rat heterotopic allograft model," *Circulation* **100**(11), 1236–1241 (1999).
- E. Gussakovskiy, O. Jilkina, Y. Yang, and V. Kupriyanov, "Hemoglobin plus myoglobin concentrations and near infrared light pathlength in phantom and pig hearts determined by diffuse reflectance spectroscopy," *Anal. Biochem.* **382**(2), 107–115 (2008).
- E. Haggblad, T. Lindbergh, M. G. Karlsson, H. Casimir-Ahn, E. G. Salerud, and T. Stromberg, "Myocardial tissue oxygenation estimated with calibrated diffuse reflectance spectroscopy during coronary artery bypass grafting," *J. Biomed. Opt.* **13**(5), 054030 (2008).
- V. V. Kupriyanov, S. Nighswander-Rempel, and B. Xiang, "Mapping regional oxygenation and flow in pig hearts *in vivo* using near-infrared spectroscopic imaging," *J. Mol. Cell. Cardiol.* **37**(5), 947–957 (2004).
- D. Baykut, M. M. Gebhard, H. Bolukoglu, K. Kadipasaoglu, S. Hennes, O. H. Frazier, and A. Krian, "Online detection of myocardial ischemia by near infrared spectroscopy with a fiberoptic catheter," *Thorac. Cardiovasc. Surg.* **49**(3), 162–166 (2001).
- A. Mayevsky, T. Manor, E. Pevzner, A. Deutsch, R. Etzioni, N. Dekel, and A. Jaronkin, "Tissue spectroscopy: a novel *in vivo* approach to real time monitoring of tissue vitality," *J. Biomed. Opt.* **9**(5), 1028–1045 (2004).
- M. Ranji, S. Kanemoto, M. Matsubara, M. A. Grosso, J. H. Gorman, 3rd, R. C. Gorman, D. L. Jaggard, and B. Chance, "Fluorescence spectroscopy and imaging of myocardial apoptosis," *J. Biomed. Opt.* **11**(6), 064036 (2006).
- M. Ranji, M. Matsubara, B. G. Leshnower, R. H. Hinmon, D. L. Jaggard, B. Chance, R. C. Gorman, and J. H. Gorman 3rd, "Quantifying acute myocardial injury using ratiometric fluorometry," *IEEE Trans. Biomed. Eng.* **56**(5), 1556–1563 (2009).
- Y. Ti and W. C. Lin, "Effects of probe contact pressure on *in vivo* optical spectroscopy," *Opt. Express* **16**(6), 4250–4262 (2008).

41. W. C. Lin, S. A. Toms, M. Motamedi, E. D. Jansen, and A. Mahadevan-Jansen, "Brain tumor demarcation using optical spectroscopy; an *in vitro* study," *J. Biomed. Opt.* **5**(2), 214–220 (2000).
42. R. N. Pittman, "*In vivo* photometric analysis of hemoglobin," *Ann. Biomed. Eng.* **14**(2), 119–137 (1986).
43. S. Prahl, "Optical absorption of hemoglobin" (1999), <http://omlc.ogi.edu/spectra/hemoglobin/>.
44. K. A. Schenkman, D. R. Marble, D. H. Burns, and E. O. Feigl, "Myoglobin oxygen dissociation by multiwavelength spectroscopy," *J. Appl. Physiol.* **82**(1), 86–92 (1997).
45. Y. Sugita, "Differences in spectra of alpha and beta chains of hemoglobin between isolated state and in tetramer," *J. Biol. Chem.* **250**(4), 1251–1256 (1975).
46. H. J. M. G. Nelissen-Vrancken, J. J. M. Debets, L. H. E. H. Snoeckx, M. J. A. P. Daemen, and J. F. M. Smits, "Time-related normalization of maximal coronary flow in isolated perfused hearts of rats with myocardial infarction," *Circulation* **93**(2), 349–355 (1996).
47. S. H. Rahimtoola, "Hibernating myocardium is hypoperfused," *Basic Res. Cardiol.* **92**, 9–11 (1997).
48. W. Ruf, G. T. Suehiro, A. Suehiro, and J. J. McNamara, "Regional myocardial blood flow in experimental myocardial infarction after pretreatment with aspirin," *J. Am. Coll. Cardiol.* **7**(5), 1057–1062 (1986).
49. B. L. Gerber, H. T. Thanh, V. Roelants, A. Pasquet, D. Vancraeynest, and J. L. J. Vanoverschelde, "Flow-function relationships in chronic left-ventricular ischemic dysfunction: Impact of the transmural extent of infarction," *J. Nucl. Cardiol.* **15**(3), 363–374 (2008).
50. R. A. Kloner and K. Przyklenk, "Stunned and hibernating myocardium," *Annu. Rev. Med.* **42**, 1–8 (1991).
51. J. L. J. Vanoverschelde, W. Wijns, M. Borgers, G. Heyndrickx, C. Depre, W. Flameng, and J. A. Melin, "Chronic myocardial hibernation in humans: from bedside to bench," *Circulation* **95**(7), 1961–1971 (1997).
52. P. Taroni, A. Pifferi, A. Torricelli, D. Comelli, and R. Cubeddu, "*In vivo* absorption and scattering spectroscopy of biological tissues," *Photochem. Photobiol. Sci.* **2**(2), 124–129 (2003).
53. C. Depre, J. L. Vanoverschelde, J. A. Melin, M. Borgers, A. Bol, J. Ausma, R. Dion, and W. Wijns, "Structural and metabolic correlates of the reversibility of chronic left ventricular ischemic dysfunction in humans," *Am. J. Physiol.* **268**(3 Pt 2), H1265–1275 (1995).
54. S. Andersson-Engels, A. Gustafson, J. Johansson, U. Stenram, K. Svanberg, and S. Svanberg, "Investigation of possible fluorophores in human atherosclerotic plaque," *Lasers Life Sci.* **5**(1–2), 1–11 (1992).
55. B. Z. Atkins, C. W. Lewis, W. E. Kraus, K. A. Hutcheson, D. D. Glower, and D. A. Taylor, "Intracardiac transplantation of skeletal myoblasts yields two populations of striated cells *in situ*," *Ann. Thorac. Surg.* **67**(1), 124–129 (1999).